Energy 44 (2012) 292–301

Contents lists available at SciVerse ScienceDirect

Energy

journal homepage: www.elsevier.com/locate/energy

Analysis of the junction temperature and thermal characteristics of photovoltaic modules under various operation conditions

Joe-Air Jiang, Jen-Cheng Wang, Kun-Chang Kuo, Yu-Li Su, Jyh-Cherng Shieh, Jui-Jen Chou*

Department of Bio-Industrial Mechatronics Engineering, National Taiwan University, No. 1, Sec. 4, Roosevelt Road, Taipei 10617, Taiwan

ARTICLE INFO

Article history:
Received 7 February 2012
Received in revised form
6 June 2012
Accepted 9 June 2012
Available online 19 July 2012

Keywords:
Junction temperature
Maximum power point (MPP)
Photovoltaic (PV) modules
p–n junction semiconductor
Solar cells
Solar irradiation

ABSTRACT

The accumulation of thermal energy in the interior of photovoltaic (PV) modules as a consequence of continuous solar irradiation causes a difference between the junction temperature of the PV modules and the ambient temperature, which leads to a serious deterioration in the performance of the PV modules. We investigate this problem in depth, proposing a novel method to directly determine the junction temperature of the PV modules based on the *p–n* junction semiconductor theory. The proposed method is a new and simple approach with a low calculation burden. Its performance is evaluated by examining the characteristics of the junction temperature of the PV modules given variation in both temperature and irradiation intensity. After obtaining the junction temperature of the PV modules, we can track a more accurate maximum power point (MPP) for the PV modules, which is inherently affected by the ambient temperature, so that the maximum utilization efficiency of PV modules can be further achieved. The experimental results demonstrate that the proposed method is a significant improvement in terms of the precision of the MPP control model, and helps PV modules produce their maximum power under various operation conditions.

1. Introduction

The use of renewable energy has gradually come to be considered a way to mitigate the negative effects brought about by global warming and climate change [1–6]. The use of renewable energy sources, such as photovoltaic (PV) energy, wind energy, and fuel cells, has been able to considerably reduce certain carbon dioxide emissions [7–13]. Many studies have made efforts to examine the performance and reliability of PV modules arising from their unique properties and suitability for various applications [14–16]. Crystalline silicon (c-Si), monocrystalline silicon (mo-Si), and polycrystalline (p-Si) PV modules are commonly considered the most reliable types of PV module technology [17–20]. However, when the PV modules are operated in an outdoor environment, with frequent fluctuations in the environmental temperature and irradiation intensity, it gives rise to critical thermal-related factors that may affect their performance and reliability of PV modules [21–24]. For example, the effects of the variation of temperature and irradiation intensity inherently lead to the deterioration in the output power of PV modules [21,23,24]. In addition, the thermal effect also influences the estimation of the maximum power point (MPP) and electrical parameters for the PV modules, such as maximum output power, maximum conversion efficiency, internal efficiency, reliability, and lifetime [21,23,24].

How to counter with the negative thermal effects on the performances of PV modules is a very important technical issue. The junction temperature, for example, is a critical parameter that significantly affects the electrical characteristics of PV modules. For practical applications of PV modules, it is very important to accurately estimate the junction temperature of PV modules and analyze the thermal characteristics of the PV modules. Once the temperature variation is taken into account, we can then acquire a more accurate MPP for the PV modules, and the maximum utilization efficiency of the PV modules can also be further achieved.

The junction temperature of the PV modules is influenced by the packaging of the PV modules and environmental factors such as ambient temperature and wind speed/direction. Under irradiation, the PV modules can directly convert solar energy into direct current (dc) electricity [25,26] which can be supplied to the load or batteries. However, for practical applications, the PV modules provide a continuous dc forward current. This may also lead to the enhancement of the self-heating effect and increase the difference between the ambient temperature and junction temperature, thereby leading to a significant deterioration in the performance of PV modules. It is reasonable to suppose that the junction

* Corresponding author. Tel.: +886 2 3366 5355; fax: +886 2 2362 7620.
E-mail address: jjchou@ntu.edu.tw (J.-J. Chou).

0360-5442/$ – see front matter © 2012 Elsevier Ltd. All rights reserved.
http://dx.doi.org/10.1016/j.energy.2012.06.029

temperature of the PV modules will fluctuate with the ambient temperature due to the significant heating caused by the dc forward current.

There have been a variety of techniques and theoretical methods used to investigate the junction temperature of the PV modules [27–32]. Usually, the junction temperature is assumed to be the module temperature, the average value of the back-side and the front-side surface temperatures [27–30]. However, it might be inaccurate to measure the junction temperature by these methods. Mattei et al. proposed a numerical method of energy balance to predict the junction temperature of PV modules [31], but this method requires complicated calculation procedures. Huang et al. developed a non-destructive method to measure the junction temperature of PV modules [32] but this depends on the quality of the data or basic parameters which are required to be determined in advance. Moreover, it must also be borne in mind that the complexity of the method does not guarantee its reliability. On the other hand, internal processes taking place within the semiconductor material during its bombardment by photons lead to the production of electricity and release the non-converted energy as heat. Focusing on the standard heat transfer mechanisms, some researchers have developed a procedure for the estimation of junction temperature which takes the relevant energy balance for the PV module into account [33–35]. However, the thermal environment which generates the instantaneous operating temperature value of the PV module is quite complex. Due to the complexity of the mathematical operations involved in the afore-mentioned methods, it is not easy to find solutions using these numerical methods without the help of a digital signal processor or a relatively powerful microcontroller. A less complicated way of determining junction temperature through a convenient estimation technique is required.

Given the shortcomings mentioned above, it is impossible to quickly acquire the junction temperature of the PV modules by using the conventional methods. This means that the accurate estimation of the junction temperature and maximum power point (MPP) for the PV modules cannot be achieved in real-time. In this study, we propose a novel method for directly determining the junction temperature of the PV modules. The proposed method is a new and simple approach with a low calculation burden. This method is developed based on the p–n junction semiconductor theory of solar cells. The junction temperature of the PV modules can be directly determined from the irradiated current–voltage characteristic curves under a variety of irradiation conditions and temperature variations. The junction temperature of the PV modules within a p–n junction diode is estimated relying on the temperature dependence of the intrinsic carrier concentration, the bandgap energy, and the effective density of states. Therefore, the proposed method is not only able to directly estimate the junction temperature of the PV modules but also able to provide a more accurate MPP for the PV modules after considering temperature and irradiation variations.

2. Theoretical basis of the proposed method

The PV modules exhibit a nonlinear current–voltage (I–V) characteristic, which varies continuously with the array temperature and solar irradiation, although there does exist one operating point where the PV modules will produce maximum power. The nonlinear I–V characteristic curve of the PV modules can be successfully explained by the p–n junction recombination mechanism for semiconductors [36]. For PV modules under illumination and connected to the load, the current I_{pv} of the PV modules, a function in terms of the voltage V_{pv}, can be expressed by the Shockley equation [21,22,36–42]:

$$I_{pv} = I_g - I_{sat}\left\{\exp\left[\frac{q(V_{pv}+I_{pv}R_s)}{nkT}\right]-1\right\} - \frac{V_{pv}+I_{pv}R_s}{R_{sh}}, \quad (1)$$

where I_g, I_{sat}, R_s, R_{sh}, and T are the experimental parameters, specifically, I_g is the light-generated photocurrent (A); I_{sat} is the ideal saturation current (A); R_s is the series resistance (ohm); R_{sh} is the parallel resistance (ohm); and T is the temperature (K). Generally, the temperature T is assumed to be the ambient temperature T_a, i.e., $T = T_a$. The q, n, and k are physical constants, where q is the electron charge (C); n is the ideality factor of the diode; and k is the Boltzmann's constant (eVK^{-1}). The ideality factor (n) of the diode is usually set as '1' when only the diffusion current flows across the junction dominates or '2' when the recombination current dominates.

It has been observed in experimental tests and practical applications that the voltage of PV modules (V_{pv}) decreases linearly with an increase in the ambient temperature and satisfies the following equation:

$$V_{pv} = V_{pv0} + C_T T_a, \quad (2)$$

where V_{pv0} is the intercept of voltage of PV modules at $T_a = 0\,^{\circ}C$; C_T is the temperature coefficient of PV module's voltage and is a negative value ($V^{\circ}C^{-1}$); and T_a is the ambient temperature. Under irradiation, the PV modules convert light energy into direct current (dc) electrical power through the p–n junction of the semiconductors to produce current and voltage [25,26]. However, the effect of the heat generated by the continuous dc current, which is affected by the packaging, thermal structure, and material properties, cannot be neglected, because it causes an inequality between the junction temperature of the PV modules and the ambient temperature. To overcome such problems, we propose a novel and simple method to directly determine the junction temperature of the PV modules from the characteristic curve given the irradiated current–voltage. Using the developed method to directly determine the junction temperature of the PV modules, we can further track a more accurate MPP, giving the PV modules a better capability to withstand temperature variations and achieve the maximum utilization efficiency of the PV modules.

In order to directly estimate the junction temperature of the PV modules based on the afore-mentioned findings, we first examine the effects of the junction temperature on the I–V curves, subject to different irradiation intensities and temperatures. The p–n junction recombination mechanism can be used to explain the linear and nonlinear temperature-dependent behaviors of semiconductor systems, such as PV modules and light-emitting diodes. Taking the temperature dependence of the semiconductor material into account, the ideal saturation current I_{sat} in the I–V characteristic of the PV modules can be expressed as [36]

$$I_{sat} = AqN_CN_V\left[\frac{1}{N_A}\sqrt{\frac{D_n}{\tau_n}}+\frac{1}{N_D}\sqrt{\frac{D_p}{\tau_p}}\right]\exp\left(\frac{-E_g}{kT}\right), \quad (3)$$

where A is the area of PV modules; N_C and N_V are the effective density of states in the conduction band and valence band, respectively; D_n and D_p are the diffusion coefficients for electrons and holes, respectively; τ_n and τ_p are the minority carrier lifetimes for electron and holes, respectively; N_D is the donor concentration; N_A is the acceptor concentration; and E_g is the bandgap energy of the semiconductor. The temperature T is usually the same as the ambient temperature T_a ($T = T_a$). The diffusion coefficients decrease when the temperature drops according to the $T^{-1/2}$ dependence, and the carrier lifetime changes with temperature due to phonon scattering [36]. In the following theoretical derivation, the dopants with concentrations of N_D and N_A are assumed to be fully ionized so

that the free carrier concentration is not temperature-dependent [36]. The effective density of states in the conduction band and valence band, N_C and N_V, are given by [36]

$$N_C \equiv 2\left(\frac{2\pi m_{de} kT_a}{h^2}\right)^{3/2} M_C, \tag{4}$$

and

$$N_V \equiv 2\left(\frac{2\pi m_{dh} kT_a}{h^2}\right)^{3/2}, \tag{5}$$

where m_{de} and m_{dh} are the density-of-state effective mass for electrons and holes, respectively; h is the Planck's constant; M_C is the number of equivalent minima in the conduction band. As the temperature increases, the energy gap of the semiconductors generally decreases [36]. Therefore, the ideal saturation current I_{sat} is strongly temperature-dependent. In the majority of practical cases, the two internal resistances R_s and R_{sh} can generally be neglected, because the series resistance R_s of the PV modules is very small and the parallel resistance R_{sh} of the PV modules is relatively high. Therefore, Eq. (1) is further simplified to

$$I_{pv} = I_g - I_{sat}\left[\exp\left(\frac{q(V_{pv})}{nkT_a}\right) - 1\right]. \tag{6}$$

For the practical operation of the PV modules, the voltage V_{pv} is greatly larger than the thermal voltage, i.e., $V_{pv} >> kT_a/q$, and Eq. (6) can be further approximated by

$$I_{pv} = I_g - I_{sat}\exp\left(\frac{qV_{pv}}{nkT_a}\right). \tag{7}$$

Next, we develop a method to investigate the influence of the thermal effect on the performance of PV modules, then use this method to estimate the temperature-dependent characteristics of the PV modules under various irradiation intensities. The derivative of the voltage V_{pv} of PV modules with respect to the ambient temperature can be expressed as

$$\frac{dV_{pv}}{dT_a} = \frac{d}{dT_a}\left[\frac{nkT_a}{q}\ln\left(\frac{I_g - I_{pv}}{I_{sat}}\right)\right], \tag{8}$$

and Eq. (8) is further manipulated to become

$$\begin{aligned}\frac{dV_{pv}}{dT_a} &= \frac{nk}{q}\ln\left(\frac{I_g - I_{pv}}{I_{sat}}\right) + \frac{nkT_a}{q}\frac{d}{dT_a}\left[\ln\left(\frac{I_g - I_{pv}}{I_{sat}}\right)\right] \\ &= \frac{nk}{q}\times\frac{qV_{pv}}{nkT_a} + \frac{nkT_a}{q}\frac{1}{I_g - I_{pv}}\frac{d(I_g - I_{pv})}{dT_a} - \frac{nkT_a}{q}\frac{1}{I_{sat}}\frac{d(I_{sat})}{dT_a}.\end{aligned} \tag{9}$$

By substituting Eqs. (3)–(5) into Eq. (9), the temperature dependence of I_{sat}, E_g, N_C and N_V is taken into account. Due to the minor contribution of the diffusion coefficients and lifetimes [36], their contribution to the temperature coefficient can be ignored. Executing the derivative in Eq. (9) yields

$$\frac{dV_{pv}}{dT_a} = \frac{qV_{pv} - nE_g}{qT_a} + \frac{n}{q}\frac{dE_g}{dT_a} - \frac{3nk}{q}. \tag{10}$$

This equation gives the fundamental temperature dependence of the voltage V_{pv}. The first summand $((qV_{pv} - nE_g)/qT_a)$, the second summand $((q/n)(dE_g/dT_a))$, and the third summand $(-3nk/q)$ on the right-hand side of Eq. (10) are due to the temperature dependence of the intrinsic carrier concentration, bandgap energy, and effective density of states N_C and N_V, respectively.

The junction temperature is a critical parameter that significantly affects the performance of PV modules, including the open-circuit voltage V_{oc}, the short-circuit current I_{sc}, the maximum output power (P_{mp}), the MPP, and the reliability. In field-test experiments on the PV modules under solar irradiation, the values of the dc forward voltage and current are measured. The heat generated by the continuous dc current leads to an extensive thermal accumulation in the interior of the PV modules, leading to the existence of a temperature difference between the junction temperature and the ambient temperature. The junction temperature for the PV modules under different output currents can be expressed as

$$T_j = T_a + \Delta T, \tag{11}$$

where T_a is the ambient temperature; and ΔT is the temperature difference between the junction temperature of the PV modules and the ambient temperature. Based on the proposed method, the derivative of the voltage V_{pv} of the PV modules with respect to the ambient temperature can be directly estimated using Eq. (10). The values of the first summand $((qV_{pv} - nE_g)/qT_a)$ and the third summand $(-3nk/q)$ on the right-hand side of Eq. (10) can be directly evaluated by substituting the values of the experimental parameters and physical constants into these two terms. However, it is difficult to obtain the detailed temperature dependence of the bandgap energy of the semiconductor. Fortunately, we can use the experiential formula to usefully characterize the second summand $((q/n)(dE_g/dT_a))$ on the right-hand side of Eq. (10) [36]. Therefore, it is feasible to apply the proposed theoretical method to directly acquire the junction temperature for practical applications of PV modules.

Using the field-test experiment and the proposed method, the junction temperatures for the PV modules under different output currents can be approximately estimated by

$$T_j = \frac{V_{pv} - V_{pv0}}{\frac{dV_{pv}}{dT_a}}, \tag{12}$$

where V_{pv} is the voltage of the PV modules; V_{pv0} is the intercept of the voltage of the PV modules at $T_a = 0\ ^\circ C$; and dV_{pv}/dT_a is the derivative of the voltage of the PV modules with respect to ambient temperature. Note that the value of V_{pv0} can be obtained from the plot of voltage versus ambient temperature. From Eq. (10), we can obtain the value of the derivative of the voltage with respect to the ambient temperature and then estimate the junction temperature of the PV modules by using Eq. (12).

Generally, PV arrays are established using modules with closer possible specifications arranged in series and/or parallel. These series-parallel-connected PV modules make up the complete power generation unit of the PV system. The performance and characteristics of individual PV modules in an array will be fairly similar under uniform irradiation patterns and considering similar values of the relevant ambient parameters around the PV array which minimize the difference among the heat transfer of different PV modules within the array. Furthermore, the junction temperature of an array can be considered as a combination of the estimated junction temperatures for individual PV modules. The proposed junction temperature estimation method is also included in the generalization from a PV module to an array of PV modules. We are able to directly and simply estimate the junction temperature of an array of PV modules with our proposed method.

Finding the MPPs of PV modules is crucial for controlling module operation under various environmental conditions. It is necessary in practical applications to track the MPP, to achieve optimal use of the available solar energy and the maximum power output can be obtained in real-time. Recently, a direct-prediction method was proposed to estimate the MPPs of PV modules

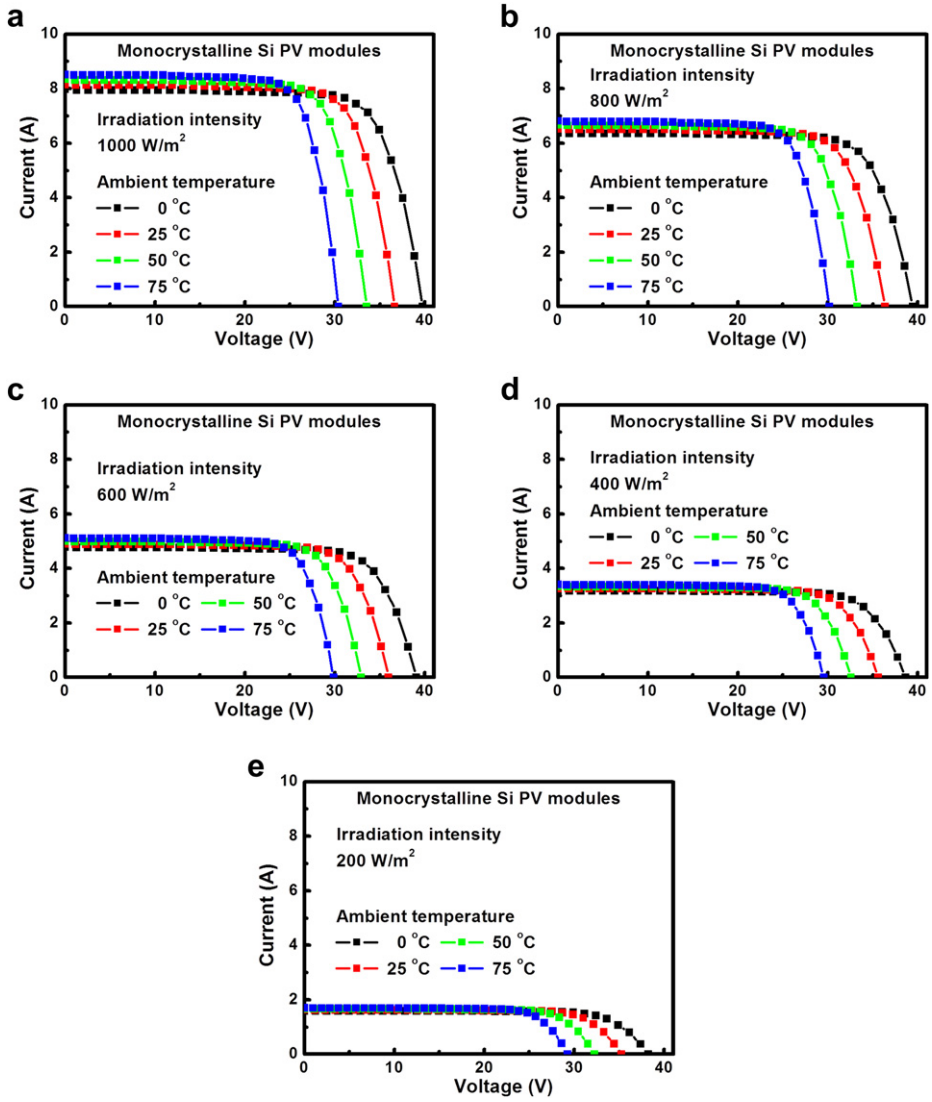

Fig. 1. The current–voltage characteristic curves of the monocrystalline Si PV modules under different ambient temperatures and irradiation intensities of (a) 1000 W/m^2, (b) 800 W/m^2, (c) 600 W/m^2, (d) 400 W/m^2, and (e) 200 W/m^2.

subject to different irradiation intensities and temperatures [21]. Using this direct-prediction method, the MPPs of PV modules can be simply and accurately determined from the irradiated I–V characteristic curve. However, the effects of the junction temperature on the MPP estimation for the PV modules were not taken into account in [21]. To further improve the accuracy of the MPP estimation, it is necessary to address this issue. According to the direct-prediction method [21], the MPPs of PV modules can be directly estimated by

$$1+\frac{q}{nkT_a}mV_{oc}-\frac{q}{nkT_a}\cdot\left(\frac{V_SI_T}{\eta mV_{oc}}\right)R_s = \exp\left[\frac{q}{nkT_a}\left(V_{oc}-mV_{oc}-\frac{V_SI_T}{\eta mV_{oc}}R_s\right)\right], \quad (13)$$

where

$$m = V_{mp}/V_{oc} \quad (14)$$

is the ratio of the voltage V_{mp} at the MPP to the open-circuit voltage V_{oc}; T_a is the ambient temperature; V_S and I_T are the root-mean-square (rms) value of the line voltage (V) and the line current (A), respectively. The MPPs of PV modules can be directly obtained in real-time using the m value calculated from the characteristic equation, Eq. (13). As the PV modules operate under various operation conditions, heat will accumulate in their interior of the PV modules, leading to a temperature difference between the junction temperature and the ambient temperature. To take the effects of the junction temperature into consideration, the ambient temperature T_a in Eq. (13) should be replaced by the junction temperature T_j to become

$$1+\frac{q}{nkT_j}mV_{oc}-\frac{q}{nkT_j}\cdot\left(\frac{V_SI_T}{\eta mV_{oc}}\right)R_s = \exp\left[\frac{q}{nkT_j}\left(V_{oc}-mV_{oc}-\frac{V_SI_T}{\eta mV_{oc}}R_s\right)\right], \quad (15)$$

where T_j is the junction temperature expressed by Eq. (11). In Eq. (15), q, n, and k are physical constants; V_{oc}, R_s, m, and η are the experimental parameters; and V_S and I_T are the measured parameters. Finally, the m value is a key parameter to be determined from the nonlinear equation, Eq. (15). The MATLAB toolbox (using a finite element method), was used to solve the nonlinear differential

equations (Eqs. (12) and (15) in this study) to obtain the T_j and m values under various operating conditions, from which the other characteristic parameters, such as V_{mp}, ΔT, and P_{mp}, etc., are obtained. Therefore, we can directly estimate the m value for the PV modules by using Eq. (15) after adjusting the temperature variation. We further obtain the V_{mp} value at the MPP using Eq. (14) so that the maximum utilization efficiency of the PV modules can be achieved.

In summary, it is easy to estimate the junction temperature of the PV modules using this method based on the p–n junction recombination mechanism. The proposed method offers a simple approach with a low calculation burden, which can be used to directly determine the junction temperature of the PV modules from their I–V characteristic curves under irradiation. The proposed method allows determination of the junction temperatures for practical applications. The junction temperatures estimated by the method can be further used to obtain a more accurate MPP for the PV modules. It is expected that the proposed method can be utilized to investigate the thermal effect on the performance of PV modules.

3. Experimental procedures

The thermal characteristic of PV modules is a critical factor which significantly affects their performance during operation. In order to investigate the thermal effect on the performance of PV modules, we conducted a number of field tests examining the temperature-dependent characteristics of the PV modules under various irradiation intensities. We used monocrystalline Si PV modules which were made up of 60 pieces of 6″ Si commercial cells connected in series to conduct the field-test experiments. The PV modules were made of p-type, monocrystalline silicon (mo-Si) wafers. The size of the PV modules was 1632 × 995 mm^2. The I–V characteristics of the monocrystalline Si PV modules were first measured under standard test conditions: an irradiation intensity of 1000 W/m^2, AM 1.5G, and ambient temperature of 25 °C. The open-circuit voltage V_{oc} and the short-circuit current I_{sc} of the monocrystalline Si PV modules were 36.84 V and 8.35 A, respectively. The conversion efficiency and the maximum output power of the monocrystalline Si PV modules were 14.16% and 230 W, respectively.

To measure the temperature-dependent current–voltage (I–V) curves, the monocrystalline Si PV modules were mounted on a sample holder stage, which was connected to a cooling system. The temperature-dependent current–voltage (I–V) curves of the monocrystalline Si PV modules were obtained from an extensive series of experiments using a solar simulator (SPI-SUN SIMULATOR 4600, Spire) under a wide ambient temperature range (0 °C–75 °C). The experiments for these field tests were conducted under four ambient temperatures (0, 25, 50, and 75 °C) and five irradiation levels with intensities of 200, 400, 600, 800, and 1000 W/m^2, respectively. Operating under different ambient temperatures and irradiation levels, we used the solar simulator to examine the I–V characteristics of the monocrystalline Si PV modules. The field-test data regarding the I–V characteristics of the monocrystalline Si PV modules were obtained using the I–V m to measure the same ten PV modules under different ambient temperatures and irradiation levels, and the test was repeated 100 times. The forward voltages of the monocrystalline Si PV modules were extracted from the I–V curves of the PV modules under various irradiation intensities and a broad ambient temperature range between 0 °C and 75 °C. The experimental data were further used to examine the feasibility of applying the proposed method to predict the MPP for PV modules. The details will be presented in next section.

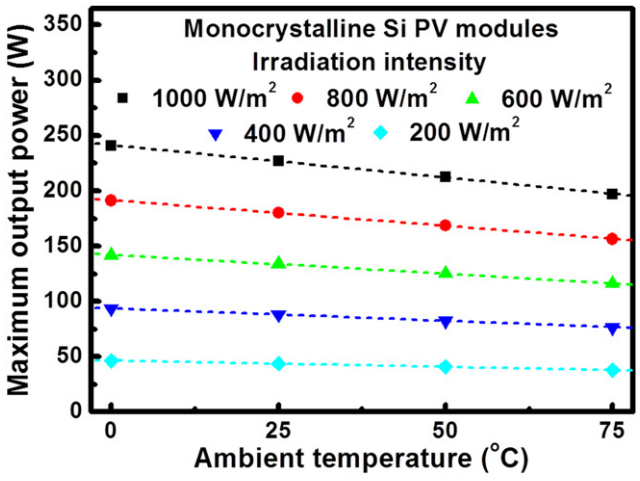

Fig. 2. The maximum output power of the monocrystalline Si PV modules expressed as a function of the ambient temperature under different irradiation intensities.

4. Results and discussion

Fig. 1(a)–(e) show the current–voltage (I–V) characteristic curves of the monocrystalline Si PV modules under different ambient temperatures and irradiation intensities of 1000 W/m^2, 800 W/m^2, 600 W/m^2, 400 W/m^2, and 200 W/m^2. From the experimental results, it is found that the changes in irradiation mainly affect the short-circuit current and output current of the PV module. However, the ambient temperature changes mainly influence the open-circuit voltage of the PV module under any of the specific intensities of solar irradiation. These experimental results are consistent with the theoretical predictions. It has been theorized that when the irradiation intensity rises, the short-circuit current I_{sc} will increase dramatically due to the increase in the minority carrier concentration, and the open-circuit voltage V_{oc} will rise due to a linear increase in the photocurrent I_{ph} [36]. An inspection of our experimental results clearly indicates that the output voltage of the PV modules decreases dramatically when the ambient temperature increases, but the output current increases slightly when the temperature rises. For example, the short-circuit currents I_{sc} of PV modules tested under an irradiation intensity of 1000 W/m^2 and ambient temperatures of 0, 25, 50, and 75 °C are approximately 7.97, 8.16, 8.34, and 8.52 A, respectively. Furthermore, as the ambient temperature increases, the open-circuit voltage V_{oc} rapidly decreases. For example, the open-circuit voltages V_{oc} of the PV modules tested under an irradiation intensity of 1000 W/m^2 and ambient temperatures of 0, 25, 50, and 75 °C are approximately 39.77, 36.65, 33.53, and 30.42 V, respectively. This phenomenon is mainly due to the exponential dependence of the saturation current I_{sat} on the temperature so that I_{sc} increases slightly [36].

Fig. 2 depicts the maximum output power of the monocrystalline Si PV modules expressed as a function of the ambient temperature under different irradiation intensities. For an ambient temperature of 25 °C, the maximum output power of PV modules decreases from 227 W to 43 W as the irradiation intensity decreases from 1000 W/m^2 to 200 W/m^2. We further investigate the influence of the thermal effect on the performance of PV modules. The maximum output power of PV modules decreases from 240 W to 196 W and from 46 W to 37 W for the PV module under an irradiation intensity of 1000 W/m^2 and 200 W/m^2, respectively, with an increase in the ambient temperature from 0 °C to 75 °C. Therefore, the overall effects of irradiation intensity and

temperature cause a reduction of power as the ambient temperature increases.

The output (or open-circuit) voltage of the PV module is mainly influenced by variations in the ambient temperature, and the output (short-circuit) current of the PV module is mainly influenced by variations in the irradiation. Thus, it is necessary to investigate the effects of the ambient temperature on the PV output voltage under different output currents and various irradiation intensities. Once this task has been completed, the relationship between the PV output voltage and the ambient temperature can be estimated. The output voltages of the monocrystalline Si PV modules under different output currents and various irradiation intensities are acquired from the *I–V* curves of the PV modules shown in Fig. 1(a)–(e). These results are plotted in Fig. 3. Fig. 3(a)–(e) shows the experimental forward voltages for the monocrystalline Si PV modules expressed as a function of the ambient temperature under different output currents and various irradiation intensities. From Fig. 3(a)–(e), we can observe that the forward voltage of PV modules decreases linearly with an increase in the ambient temperature even if the experimental condition combinations of irradiation intensities and output currents are changed. In the experiments when the output current is 0.5 A, if the experimental irradiation intensities are varied with an equal decrement (i.e., 200 W/m^2) from 1000 W/m^2 to 200 W/m^2, the forward voltages of PV modules under varying ambient temperatures from 0 °C to 75 °C will show an approximate shift downward from 39.52 V to 30.24 V, from 39.14 V to 29.96 V, from 38.65 V to 29.59 V, from 38.06 V to 29.14 V, and from 37.01 V to 28.38 V, respectively. The drops in the forward voltages of PV modules ranged from 9.28 V to 8.63 V. This implies that the forward voltages of PV modules are slightly affected by a wide range of variation in irradiation and ambient temperature. It also reveals that the forward voltages of PV modules will slightly decrease with the decrease in the irradiation intensity under any specific experimental condition combinations of ambient temperature and output current. On the other hand, a careful inspection of Fig. 3(a)–(e) clearly indicates that if the PV module operates under a specific combination of irradiation and ambient temperature, the forward voltages of the monocrystalline Si PV modules exhibit a significant down shift when the output current of the PV module increases. In the case of the experimental condition combination (irradiation, ambient temperature) = (1000 W/m^2, 25 °C), for instance, the

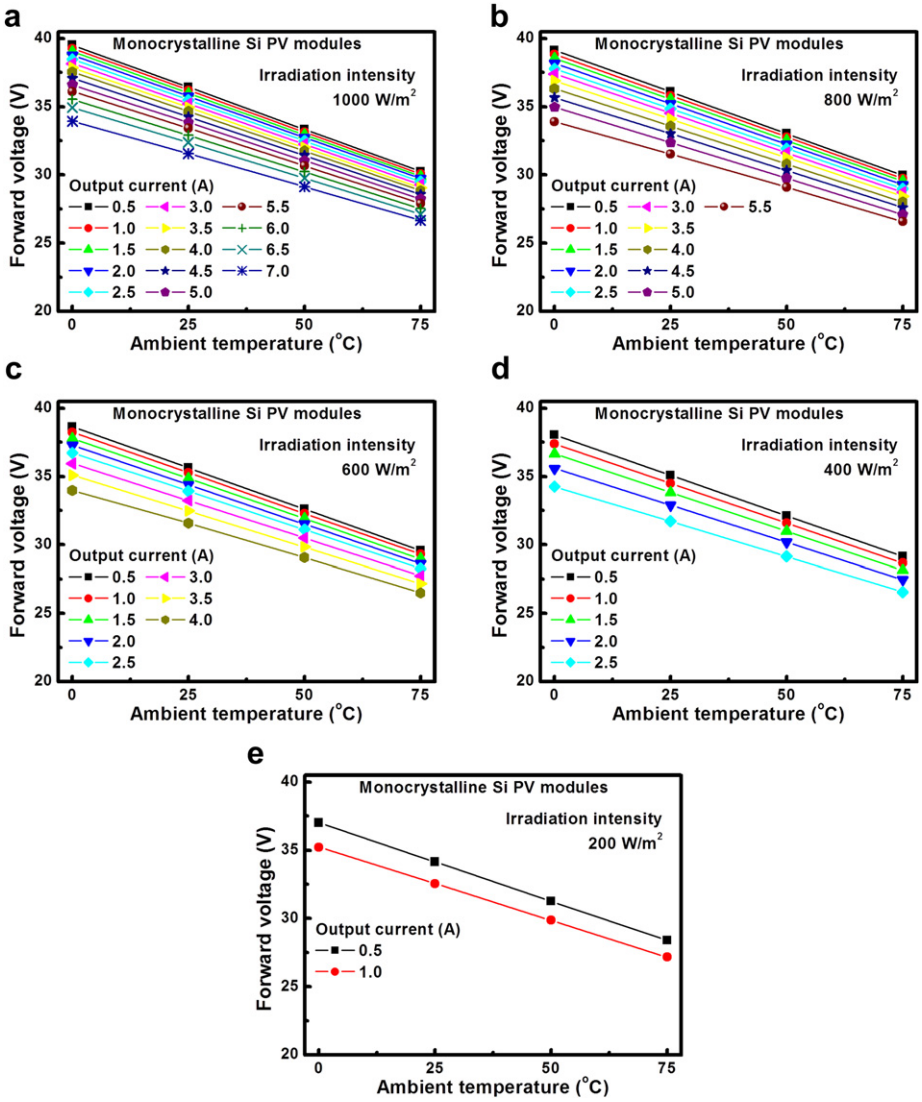

Fig. 3. The experimental forward voltage of the monocrystalline Si PV modules expressed as a function of the ambient temperature under different output currents and irradiation intensities of (a) 1000 W/m^2, (b) 800 W/m^2, (c) 600 W/m^2, (d) 400 W/m^2, and (e) 200 W/m^2.

forward voltages of the tested PV modules will be down shifted from 36.43 V to 31.56 V when the PV module's output current increases from 0.5 A to 7.0 A. This phenomenon might be attributable to the relationship between the forward voltage of the PV modules and the temperature dependence of the saturation current I_{sat} under a constant irradiation intensity [36].

The experimental results also revealed that the linear relationship between the experimental voltage of the PV modules and ambient temperature is consistent with that described by Eq. (2). However, the temperature coefficient of the voltage (C_T, as indicated by the slopes of the straight lines shown in Fig. 3(a)–(e)) was slightly affected by the significant self-heating effect and thermal accumulation of the PV modules under irradiation [27–35]. Therefore, it is difficult to directly and accurately estimate the value of C_T, so that the ambient temperature cannot adequately represent the junction temperature.

The proposed junction temperature estimation method can be used to obtain the values of the V_{pv0} from the plots of voltage versus temperature, as shown in Fig. 3(a)–(e), and the derivative of the voltage V_{pv} of the PV modules with respect to ambient temperature (dV_{pv}/dT_a) can be directly estimated by Eq. (10). Usually, the output current of the PV module is closely related to its V_{pv} and V_{pv0}; both values of V_{pv} and V_{pv0} will further affect the estimation of the junction temperature T_j. Therefore, once the values of V_{pv0} and dV_{pv}/dT_a are available, the junction temperature of the PV modules and the dependence of the junction temperatures on different output currents can be further indirectly estimated using Eq. (12) and the data from field-test experiments shown in Fig. 3(a)–(e). Fig. 4(a)–(e) shows the junction temperatures of monocrystalline Si PV modules plotted as a function of the ambient temperature for different combinations of output currents and irradiation intensities. These figures indicate a significant upward or downward shift in the junction temperature of the PV modules depending on their operating output current when operated at any specific combination of irradiation and ambient temperature. It can be seen from Fig. 4(a)–(e) that the junction temperatures of the monocrystalline Si PV modules under a constant irradiation intensity will vary linearly with an increase in the ambient temperature, even if the operated output currents of the PV modules are changed. For example, in the case where the output current is 5 A, the junction temperature T_j under an irradiation of 1000 W/m^2 and ambient temperatures of 0, 25, 50, and 75 °C will gradually increase to approximately 32.95, 57.77, 82.78, and 107.95 °C, respectively. As mentioned above, both the shift in the forward voltage and the

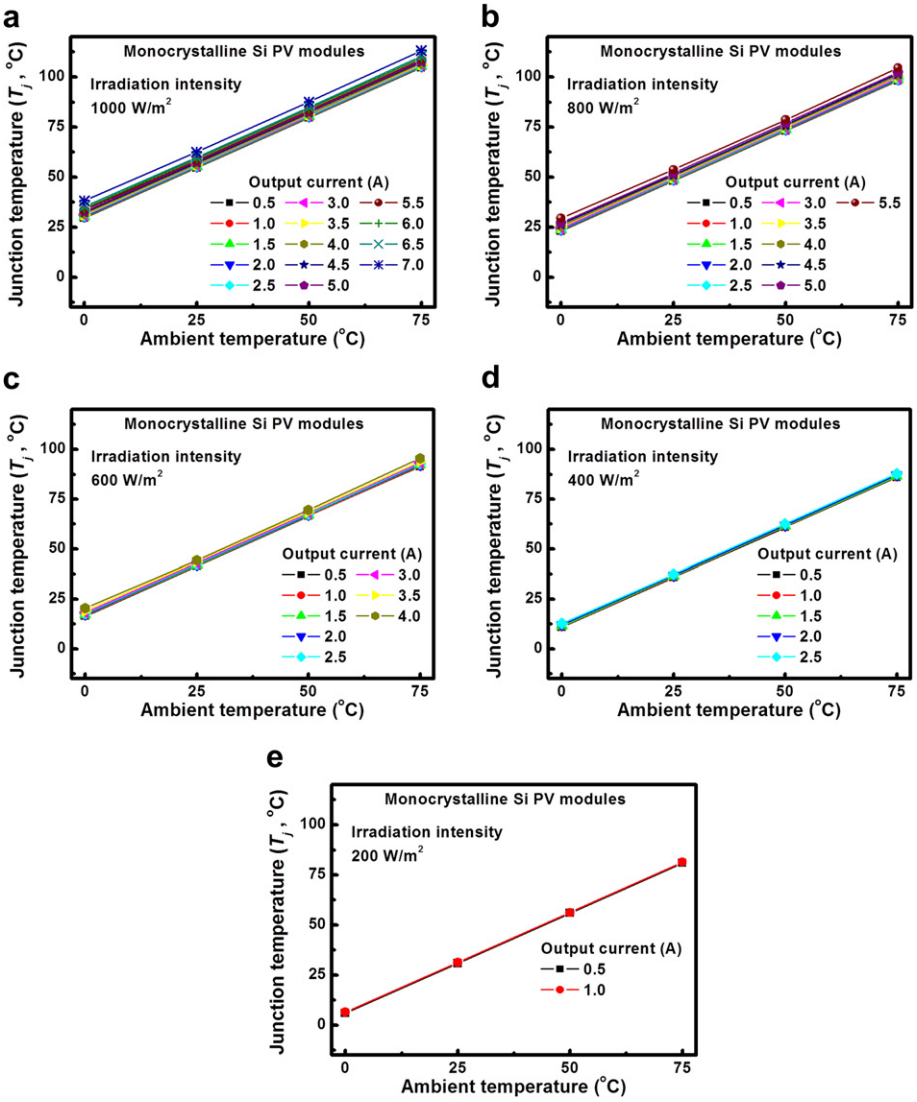

Fig. 4. The junction temperatures of the monocrystalline Si PV modules expressed as a function of the ambient temperature under different output currents and irradiation intensities of (a) 1000 W/m^2, (b) 800 W/m^2, (c) 600 W/m^2, (d) 400 W/m^2, and (e) 200 W/m^2.

increase in the junction temperature that correspond to the increase in the ambient temperature arise mainly because of the contact resistance between the metal and the Si layers and the bandgap shrinkage effect [36]. On the other hand, when the PV modules operate under an irradiation of 1000 W/m^2 but the output current remains 3 A, the junction temperature T_j increases significantly to approximately 31.02, 55.96, 80.96, and 106.02 °C with an increase in the ambient temperature from 0 °C to 75 °C, respectively. It is also revealed that there will be a significant decrease in the junction temperatures of PV modules with the decrease in the operating output current under a specific combination of irradiation intensity and ambient temperature. For example, for the combination of (irradiation, ambient temperature) = (1000 W/m^2, 25 °C), the junction temperature T_j shift from 54.66 °C to 62.54 °C as the output current of the tested PV module changes from 0.5 A to 7.0 A. This notable shift phenomenon in the junction temperature T_j depending on the output current is quite similar to that observed when examining the forward voltage of the PV modules. It is worth noting that there is slight increase in the junction temperature of monocrystalline Si PV modules under a specific irradiation intensity when the output current increases. Furthermore, a careful examination of the data in Fig. 4(a)–(e) also reveals that the junction temperatures of PV modules will decrease with the decrease in irradiation intensity for a specific combination of operating output current and ambient temperature. For example, suppose that the PV module provides an operating output current of 1 A when the ambient temperatures is 25 °C and the irradiation intensities are 1000 W/m^2, 800 W/m^2, 600 W/m^2, 400 W/m^2, and 200 W/m^2. In this case, the junction temperatures of the tested PV module are approximately 54.88, 48.36, 41.69, 36.15, and 31.25 °C, respectively. From this it can be seen that the junction temperature of PV modules will be significantly affected by the various operation conditions such as the irradiation intensity and ambient temperature.

Through analysis of the junction temperatures of monocrystalline Si PV modules shown in Fig. 4(a)–(e), we can also obtain the dependence of the irradiation intensity on the junction temperatures of the PV module for different ambient temperatures. The results are plotted in Fig. 5(a). It should be noted that the PV modules will not absorb light energy and will not generate any heat in their interior when exposed to an irradiation intensity of 0 W/m^2. It is reasonable to suppose that the junction temperature of the PV modules will be equal to the ambient temperature when the irradiation intensity is 0 W/m^2. The figure shows that there is a stepwise rise in the junction temperatures of the PV modules when the ambient temperature increases in equal increments for each experimental run, i.e., 25 °C. This might be primarily attributable to the contact resistance and the bandgap shrinkage effect [36]. Furthermore, the junction temperature of the PV modules increases linearly under a constant ambient temperature with the rising of the irradiation intensity, as depicted in Fig. 5(a). For example, the junction temperatures T_j under an ambient temperature of 25 °C and irradiations of 0, 200, 400, 600, 800, and 1000 W/m^2 are approximately 25.00, 31.07, 36.57, 42.64, 49.98, and 57.11 °C, respectively. This can be attributed to the heat generated by the continuous dc current and thermal accumulation in the interior of the PV modules under irradiation. Moreover, when the PV modules operate under an irradiation of 1000 W/m^2, the junction temperature T_j will increase significantly with increasing ambient temperature from 0 °C to 75 °C to approximately 32.28, 57.11, 82.12, and 107.28 °C, respectively. The results indicate that there is a gradually linear increase in the junction temperature of the PV modules under a constant irradiation intensity with the increase of the ambient temperature. The error bars in Fig. 5(a) represent the standard deviation of the junction temperatures of the monocrystalline Si PV modules estimated by the junction temperature estimation method. Generally, the stronger the experimental radiation is, the greater the standard deviation obtained. Under higher irradiation intensity, the PV modules can directly convert solar energy into dc electricity and continuously provide a larger forward current. The larger dc current leads to a gradual increase in the heat generated in the interior of the PV modules. The packaging thermal structure and material properties cause greater variation in the junction temperature of PV modules. Therefore, the standard deviations of the junction temperatures of the monocrystalline Si PV modules under higher irradiation intensities are larger than under lower irradiation intensities. In the case of an irradiation of 1000 W/m^2, for instance, the standard deviations of the estimated PV module's junction temperatures with respect to the four testing temperatures from 0 to 75 °C will be 2.35 °C, 2.17 °C, 2.18 °C, and 2.34 °C, respectively. These standard deviations are quite small. This indicates that the estimated junction temperature of the PV modules obtained with the proposed junction temperature estimation method is very stable with little deviation.

Next, we further investigate the effect of various levels of irradiation on the temperature difference ΔT of the PV modules. The temperature differences $\Delta T = T_j - T_a$ are estimated under different ambient temperatures from 0 to 75 °C. Fig. 5(b) shows the temperature differences (ΔT) for the monocrystalline Si PV module expressed as a function of the irradiation intensities under different ambient temperatures. The averaged temperature differences ΔT and the standard deviation of the junction temperature of the PV modules at an increment of 200 W/m^2 in the irradiation intensities

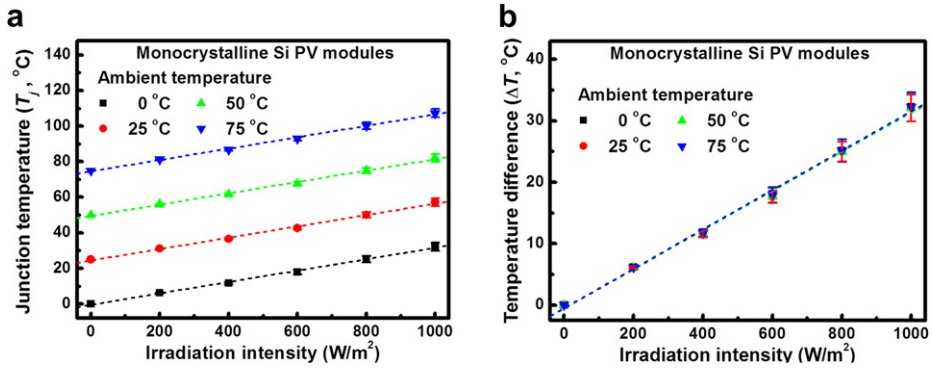

Fig. 5. The thermal characteristic curves of the monocrystalline Si PV modules: (a) junction temperatures; and (b) temperature differences for the monocrystalline Si PV modules expressed as a function of the irradiation intensity under different ambient temperatures. The error bars indicate the standard deviation of the junction temperatures of the monocrystalline Si PV modules estimated by the junction temperature method.

Table 1
The thermal dependence of the V_{mp}/V_{oc} for the monocrystalline Si PV modules and the prediction error $|V_{mp}/V_{oc}|$ (%) obtained with the proposed estimation method under different irradiation intensities and ambient temperatures.

Irradiation intensity	Ambient temperature	Experimental results	Direct-prediction method ([21] [a])		Direct-prediction method with an adjustment of T_j	
(W/m^2)	(°C)	V_{mp}/V_{oc}	V_{mp}/V_{oc} [b]	Prediction error: $\lvert V_{mp}/V_{oc}\rvert$ (%)	V_{mp}/V_{oc} [b]	Prediction error: $\lvert V_{mp}/V_{oc}\rvert$ (%)
1000	0	0.8145	0.8531	4.74	0.8206	0.75
	25	0.8144	0.8362	2.68	0.8192	0.59
	50	0.8137	0.8171	0.42	0.8168	0.38
	75	0.8133	0.7974	1.95	0.8152	0.23
800	0	0.8145	0.8521	4.62	0.8184	0.48
	25	0.8144	0.8352	2.55	0.8171	0.33
	50	0.8137	0.8161	0.29	0.8142	0.06
	75	0.8133	0.7964	2.08	0.8101	0.39
600	0	0.8145	0.8513	4.52	0.8172	0.33
	25	0.8144	0.8342	2.43	0.8152	0.10
	50	0.8137	0.8152	0.18	0.8131	0.07
	75	0.8133	0.7954	2.20	0.8089	0.54
400	0	0.8145	0.8501	4.37	0.8162	0.21
	25	0.8144	0.8331	2.30	0.8146	0.02
	50	0.8137	0.8149	0.15	0.8133	0.05
	75	0.8133	0.7938	2.40	0.8085	0.59
200	0	0.8145	0.8489	4.22	0.8151	0.07
	25	0.8144	0.8318	2.14	0.8141	0.04
	50	0.8137	0.8145	0.10	0.8131	0.07
	75	0.8133	0.7932	2.47	0.8081	0.64

[a] The V_{mp}/V_{oc} and $|V_{mp}/V_{oc}|$ (%) of the monocrystalline Si PV modules were estimated by the direct-prediction method [21] without an adjustment of the junction temperature T_j.
[b] The values of the open-circuit voltage (V_{oc}) used are the same as the experimental values.

ranging from 200 to 1000 W/m^2 are 6.13 ± 0.2 °C, 11.6 ± 0.6 °C, 17.7 ± 1.1 °C, 25.1 ± 1.7 °C, and 32.2 ± 2.2 °C, respectively. These experimental results show that the method presented here is stable and is easy to use. Furthermore, it can be seen that the ΔT of the PV modules rises due to the increase in the irradiation intensity but remains almost the same when the ambient temperature is altered. From the experimental results, we also find that ΔT is almost linearly proportional to the irradiation intensity under various ambient temperatures. This suggests that the difference between the junction temperature of the PV modules and the ambient temperature is mainly influenced by the irradiation intensity but is quite insensitive to changes in the ambient temperature.

Generally, I_{mp} and V_{mp} are utilized to represent the current and voltage of PV modules operated in the maximum power output mode, i.e., the MPP consists of I_{mp} and V_{mp}. During PV modules operation, the MPPs of PV modules are deeply affected by the environmental conditions such as irradiation intensity and ambient temperature. Usually, the MPPs of PV modules can be tracked accurately using traditional methods, such as the lookup table method [43,44], perturb-and-observe method [45–48], and incremental conductance method [49,50]. However, these methods did not take the thermal effect into consideration. Therefore, the proposed junction temperature estimation method can be used to determine the MPPs of PV modules more accurately. Following the treatment in our previous work [21], the thermal dependence of the V_{mp}/V_{oc} for the monocrystalline Si PV modules and the prediction error of the proposed estimation method under different combinations of irradiation intensities and ambient temperatures are listed in Table 1. There are three kinds of V_{mp}/V_{oc} values for the monocrystalline Si PV modules listed in Table 1. The first ones come from the experimentally measured data; the second ones are estimated by the direct-prediction method [21] without an adjustment of the junction temperature T_j; and the third ones are the data estimated by the method proposed in this work taking adjustment of the junction temperature T_j into account. By using Eq. (15), the effects of temperature variations on the junction temperatures have been taken into consideration so that we can directly estimate the V_{mp} at the MPPs of the PV modules. After substituting the junction temperature adjustment into the proposed direct-prediction MPP method, with an increase in irradiation intensity from 200 to 1000 W/m^2, the average percentage of prediction error for $|V_{mp}/V_{oc}|$ (%) at the MPPs of PV modules will respectively decrease from 2.23%, 2.30%, 2.33%, 2.39%, and 2.45%–0.21%, 0.22%, 0.26%, 0.32%, and 0.49%. Clearly, the error for estimating the MPPs of PV modules is significantly reduced by using our new method. The experimental results indicate that the proposed junction temperature estimation method can be used to accurately estimate the MPPs of the PV modules under environmental variations. Therefore, the proposed method is an effective and simple way to determine the temperature differences of PV modules from the irradiated I–V characteristic curves even for changing ambient temperatures.

In summary, this study confirms that the junction temperature of the PV modules can be simply and stably estimated using the junction temperature estimation method. This method can also be easily integrated with the direct-prediction MPP method to develop control rules for maximum power point tracking (MPPT) methods and applied to PV generation systems.

5. Conclusions

In this study, we investigated the effectiveness of the proposed junction temperature estimation method for PV modules subject to different irradiation intensities and ambient temperatures. Based on the p–n junction recombination mechanism, we are able to simply estimate the junction temperature of the PV modules with our proposed method. It has been found that the junction temperature of the PV modules gradually increases as the radiation intensity and ambient temperature increase. Furthermore, the temperature difference between the junction temperature and the ambient temperature will increase linearly with an increase in the radiation intensity, even if the ambient temperature changes. In order to investigate the influence of the temperature effect on the accuracy of MPP and $|V_{mp}/V_{oc}|$ (%) estimations, we conducted a series of experiments, including field data tests and numerical estimation, to evaluate the performance of the proposed junction

temperature estimation method. The effectiveness of the proposed method is verified through experiments conducted under various weather conditions. Combining the direct-prediction MPP method with the new proposed junction temperature estimation method for PV modules, we are able to reduce the average percentage of prediction error $|V_{mp}/V_{oc}|$ (%) at the MPPs of the PV modules from 2.23%, 2.30%, 2.33%, 2.39%, and 2.45%–0.21%, 0.22%, 0.26%, 0.32%, and 0.49%, respectively, as irradiation intensities increase in an equal increment of 200 W/m^2 from 200 to 1000 W/m^2. The results indicate that the proposed method can provide a more accurate estimation of the MPPs of PV modules under environmental variations while obtaining the maximum power output for practical applications.

Acknowledgments

This work was financially supported in part by the National Science Council, the President of National Taiwan University, and the Council of Agriculture of the Executive Yuan, Taiwan, under the grants: NSC 100-2218-E-002-005, NSC 100-2218-E-002-006, NSC 100-3113-E-002-005, NSC 100-3113-P-002-012, NSC 101-3113-E-002-005, NSC 101-ET-E-002-012-ET, 10R70606-4, 101AS-7.1.2-BQ-B1, and 101AS-7.1.2-BQ-B2. The authors are deeply grateful to Mrs. Debbie Nester for her great help in English editing. We are also grateful to the Editor and the anonymous referees for their invaluable suggestions to improve the paper.

References

[1] Arent DJ, Wise A, Gelman R. The status and prospects of renewable energy for combating global warming. Energ Econ 2011;33:584–93.
[2] Keith DW, DeCarolis JF, Denkenberger DC, Lenschow DH, Malyshev SL, Pacala SN, et al. The influence of large-scale wind power on global climate. Proc Natl Acad Sci U S A 2004;101:16115–20.
[3] Wang C, Prinn RG. Potential climatic impacts and reliability of very large-scale wind farms. Atmos Chem Phys 2010;10:2053–61.
[4] Zhang X, Zhao X, Smith S, Xu J, Yu X. Review of R&D progress and practical application of the solar photovoltaic/thermal (PV/T) technologies. Renew Sustain Energ Rev 2012;16:599–617.
[5] Andrei H, Dogaru-Ulieru V, Chicco G, Cepisca C, Spertino F. Photovoltaic applications. J Mater Process Technol 2007;181:267–73.
[6] Edmonds I, Smith G. Surface reflectance and conversion efficiency dependence of technologies for mitigating global warming. Renew Energ 2011;36:1343–51.
[7] Sakaki K, Yamada K. CO_2 mitigation by new energy systems. Energ Convers Manag 1997;38:S655–60.
[8] Yamada K, Komiyama H, Kato K, Inaba A. Evaluation of photovoltaic energy systems in terms of economics, energy, and CO_2 emissions. Energ Convers Manag 1995;36:819–22.
[9] Abdullah MO, Yung VC, Anyi M, Othman AK, Abdul Hamid KB, Tarawe J. Review and comparison study of hybrid diesel/solar/hydro/fuel cell energy schemes for a rural ICT telecenter. Energy 2010;35:639–46.
[10] Lau KY, Yousof MFM, Arshad SNM, Anwari M, Yatim AHM. Performance analysis of hybrid photovoltaic/diesel energy system under Malaysian conditions. Energy 2010;35:3245–55.
[11] Bayod-Rújula ÁA, Lorente-Lafuente AM, Cirez-Oto F. Environmental assessment of grid connected photovoltaic plants with 2-axis tracking versus fixed modules systems. Energy 2011;36:3148–58.
[12] Singh GK. Modeling and analysis of six-phase synchronous generator for stand-alone renewable energy generation. Energy 2011;36:5621–31.
[13] Wissem Z, Gueorgui K, Hédi K. Modeling and technical–economic optimization of an autonomous photovoltaic system. Energy 2012;37:263–72.
[14] Takigawa K, Okada N, Kuwabara N, Kitamura A, Yamamoto F. Development and performance test of smart power conditioner for value-added PV application. Sol Energ Mater Sol Cells 2003;75:547–55.
[15] Sopitpan S, Changmuang P, Panyakeow S. Monitoring and data analysis of a PV system connected to a grid for home applications. Sol Energ Mater Sol Cells 2001;67:481–90.
[16] Close J, Ip J, Lam KH. Water recycling with PV-powered UV-LED disinfection. Renew Energ 2006;31:1657–64.
[17] Huld T, Friesen G, Skoczek A, Kenny RP, Sample T, Field M, et al. A power-rating model for crystalline silicon PV modules. Sol Energ Mater Sol Cells 2011;95:3359–69.
[18] Sastry OS, Saurabh S, Shil SK, Pant PC, Kumar R, Kumar A, et al. Performance analysis of field exposed single crystalline silicon modules. Sol Energ Mater Sol Cells 2010;94:1463–8.
[19] Park KE, Kang GH, Kim HI, Yu GJ, Kim JT. Analysis of thermal and electrical performance of semi-transparent photovoltaic (PV) module. Energy 2010;35:2681–7.
[20] Alsema EA, de Wild-Scholten MJ. The real environmental impacts of crystalline silicon PV modules: an analysis based on up-to-date manufacturers data. In. Presented at the 20th European photovoltaic energy research conference and exhibition, Barcelona, Spain; 2005.
[21] Wang JC, Su YL, Shieh JC, Jiang JA. High-accuracy maximum power point estimation for photovoltaic arrays. Sol Energ Mater Sol Cells 2011;95:843–51.
[22] Wang JC, Shieh JC, Su YL, Kuo KC, Chang YW, Liang YT, et al. A novel method for the determination of dynamic resistance for photovoltaic modules. Energy 2011;36:5968–74.
[23] Kuo YC, Liang TJ, Chen JF. Novel maximum-power-point-tracking controller for photovoltaic energy conversion system. IEEE Trans Ind Electron 2001;48:594–601.
[24] Mutoh N, Ohno M, Inoue T. A method for MPPT control while searching for parameters corresponding to weather conditions for PV generation systems. IEEE Trans Ind Electron 2006;53:1055–65.
[25] Borowy BS, Salameh ZM. Methodology for optimally sizing the combination of a battery bank and PV array in a wind/PV hybrid system. IEEE Trans Energ Convers 1996;11:367–75.
[26] Rauschenbach HS. Solar cell array design handbook: the principles and technology of photovoltaic energy conversion. New York: Van Nostrand Reinhold Co; 1980.
[27] Skoplaki E, Palyvos JA. Operating temperature of photovoltaic modules: a survey of pertinent correlations. Renew Energ 2009;34:23–9.
[28] Mondol JD, Yohanis YG, Smyth M, Norton B. Long-term validated simulation of a building integrated photovoltaic system. Sol Energ 2005;78:163–76.
[29] Mondol JD, Yohanis YG, Norton B. Comparison of measured and predicted long term performance of a grid connected photovoltaic system. Energ Convers Manag 2007;48:1065–80.
[30] Mondol JD, Yohanis YG, Norton B. The effect of low insolation conditions and inverter oversizing on the long-term performance of a grid-connected photovoltaic system. Prog Photovoltaics 2007;15:353–68.
[31] Mattei M, Notton G, Cristofari C, Muselli M, Poggi P. Calculation of the polycrystalline PV module temperature using a simple method of energy balance. Renew Energ 2006;31:553–67.
[32] Huang BJ, Yang PE, Lin YP, Lin BY, Chen HJ, Lai RC, et al. Solar cell junction temperature measurement of PV module. Sol Energ 2011;85:388–92.
[33] Tiwari A, Sodha MS. Performance evaluation of a solar PV/T system: an experimental validation. Sol Energ 2006;80:751–9.
[34] King DL, Kratochvil JA, Boyson WE, Bower W. Field experience with a new performance characterization procedure for photovoltaic arrays. In. Proceedings of the second world conference and exhibition on photovoltaic solar energy conversion, Vienna, Austria; 1998. p. 1947–52.
[35] Ingersoll JG. Simplified calculation of solar cell temperatures in terrestrial photovoltaic arrays. J Sol Energ Eng Trans-ASME 1986;108:95–101.
[36] Sze SM, Ng KK. Physics of semiconductor devices. 3rd ed. New York: Wiley; 2006.
[37] Bose BK, Szczesny PM, Steigerwald RL. Microcomputer control of a residential photovoltaic power conditioning system. IEEE Trans Ind Appl 1985;IA-21:1182–91.
[38] Hua CC, Lin JR, Shen CM. Implementation of a DSP-controlled photovoltaic system with peak power tracking. IEEE Trans Ind Electron 1998;45:99–107.
[39] Kaushika ND, Rai AK. An investigation of mismatch losses in solar photovoltaic cell networks. Energy 2007;32:755–9.
[40] Tina GM, Rosa-Clot M, Rosa-Clot P, Scandura PF. Optical and thermal behavior of submerged photovoltaic solar panel: SP2. Energy 2012;39:17–26.
[41] Gautam NK, Kaushika ND. An efficient algorithm to simulate the electrical performance of solar photovoltaic arrays. Energy 2002;27:347–61.
[42] Liao CC. Genetic k-means algorithm based RBF network for photovoltaic MPP prediction. Energy 2010;35:529–36.
[43] Hiyama T, Kouzuma S, Imakubo T. Identification of optimal operating point of PV modules using neural network for real time maximum power tracking control. IEEE Trans Energ Convers 1995;10:360–7.
[44] Hiyama T, Kitabayashi K. Neural network based estimation of maximum power generation from PV module using environmental information. IEEE Trans Energ Convers 1997;12:241–7.
[45] Sullivan CR, Powers MJ. A high-efficiency maximum power point tracker for photovoltaic arrays in a solar-powered race vehicle. In. Proc IEEE power electronics specialists conference; 20–24 June 1993, Seattle, WA, USA. p. 574–80.
[46] Gow JA, Manning CD. Controller arrangement for boost converter systems sourced from solar photovoltaic arrays or other maximum power sources. In: Proc inst electr eng–electr power appl, vol. 147; 2000. p. 15–20.
[47] Enslin JHR, Wolf MS, Snyman DB, Sweigers W. Integrated photovoltaic maximum power point tracking converter. IEEE Trans Ind Electron 1997;44:769–73.
[48] Shoeman JJ, Wyk JD. A simplified maximal power controller for terrestrial photovoltaic panel arrays. In. Proc IEEE power electronics specialists conference; 14–17 June 1982, Cambridge, MA, USA. p. 361–7.
[49] Wasynzczuk O. Dynamic behavior of a class of photovoltaic power systems. IEEE Trans Power App Syst 1983;PAS-102:3031–7.
[50] Hussein KH, Muta I, Hoshino T, Osakada M. Maximum photovoltaic power tracking: an algorithm for rapidly changing atmosphere conditions. In: Proc inst elect eng–gener transmiss distrib, vol. 142; 1995. p. 59–64.